Method Transfer from High Pressure Liquid Chromatography to Ultra High Pressure Liquid Chromatography using a Solid Theoretical Basis. I. A Thermodynamic Perspective

Dennis Åsberg, Marek Leśko, Jörgen Samuesson, Krzysztof Kaczmarski and Torgny Fornstedt*

[1] Department of Engineering and Chemical Sciences, Karlstad University, SE-651 88 Karlstad, Sweden

[2] Department of Chemical Engineering, Rzeszów University of Technology, PL-35 959 Rzeszów, Poland

* Corresponding author's information:
Torgny Fornstedt, Professor, Karlstad University, SE-651 88 Karlstad, Sweden
Torgny.Fornstedt@kau.se, +46 54 700 1960; + 46 73 271 28 90

Abstract

This is the first investigation in a series that aims to enhance the scientific knowledge needed for reliable analytical method transfer between HPLC and UHPLC using the Quality by Design (QbD) framework. Here, we investigated the differences and similarities from a thermodynamic point of view between RP-LC separations conducted with 3.5 µm (HPLC) respective 1.7 µm (UHPLC) C18 particles. Three different model solutes and one pharmaceutical compound were used: the uncharged cycloheptanone, the cationic benzyltriethylammonium chloride, the anionic sodium 2-naphatlene sulfonate and the pharmaceutical compound omeprazole, which was anionic at the studied pH. Adsorption data were determined for the four solutes at varying fractions of organic modifier and in gradient elution in both the HPLC and UHPLC system, respectively. From the adsorption data, the adsorption energy distribution of each compound was calculated and the adsorption isotherm model was estimated. We found that the adsorption energy distribution was similar; with only minor differences in degree of homogeneity, for HPLC and UHPLC stationary phases The adsorption isotherm model did not change between HPLC and UHPLC, but the parameter values changed considerably especially for the ionic compounds. The dependence of the organic modifier followed the same trend in HPLC as in UHPLC. These results indicates that the adsorption mechanism of a solute is the same on HPLC and UHPLC stationary phases which simplifies design of a single analytical method applicable to both HPLC and UHPLC conditions within the QbD framework.

Keywords: HPLC; UHPLC; Quality by design; Adsorption isotherm; Gradient elution; Omeprazole

1 Introduction

Ultra-High Pressure Liquid Chromatography (UHPLC) instrumentation became commercially available in 2004 (Waters Acquity UPLC) and now most instrument manufactures offers UHPLC equipment [1].

UHPLC provides faster separations with lower solvent consumptions as compared to HPLC, with preserved column efficiency [1,2]; therefore the interest from the pharmaceutical industry has grown steadily the last years [3–8]. UHPLC is now well-established and the pharmaceutical industry wants to transfer their HPLC methods to UHPLC without costly post regulatory changes [9]. Today, many pharmaceutical companies file both an HPLC and an UHPLC method. However, the traditional process of getting an analytical method approved by the regulators is extremely tedious and time-consuming. However, the design of analytical methods within the Quality by Design (QbD) framework allow changes from HPLC to UHPLC to be made without re-filing a new method if the changes are within the design space [10]. The idea of QbD is to design methods through scientific understanding rather than empirical know-how [11]. It is therefore of utmost importance to have clear scientific understanding of the design space the method has been developed for, i.e. in this case the differences between HPLC and UHPLC, which is the focus of this investigation.

From an instrumental perspective the main difference between HPLC and UHPLC is that smaller particles are used in the column packing material in UHPLC; as a consequence pumps able to manage pressures up to 1000 bar are required. This results in at least three factors that can affect the chromatographic behavior (retention, efficiency, resolution, etc.); (i) although the column manufactures aim to produce columns with the same column chemistry in HPLC and UHPLC, the reduced particle size can results in different ligand density distribution, porosity, relative particle size distribution etc. (ii) the retention time and resolution changes with pressure [12,13] and (iii) due to viscous friction, temperature gradients arise in the column which can affect both retention and efficiency [14,15]. The dwell volume of the system and the extra-column volume are also generally smaller in an UHPLC system.

Omeprazole (“OM”), an important proton pump inhibitor [16,17] used in the treatment of heartburn and stomach ulcers , together with three model compounds are investigated in realistic conditions, i.e. gradient elution and buffered mobile phases. The three model compounds are one uncharged (cycloheptanone, “C7”), one negatively charged (sodium 2-naphatlene sulfonate, “SNS”) and one positively charged (benzyltriethylammonium chloride, “BTEAC”). This study is part of a longer project where the overreaching aim is to discuss how the major differences between HPLC and UHPLC conditions affect the adsorption equilibrium and give guidelines that can be of use when transferring a method from HPLC to UHPLC using QbD in a pharmaceutical environment.

This study aims at a detailed in-depth investigation on the similarities and differences between typical modern HPLC and UHPLC operational conditions, respectively, with focus on the thermodynamics of the adsorption equilibrium; the flow rate in UHPLC is kept low for avoiding temperature gradients and ensure accurate adsorption isotherm determinations. Such a fundamental comparison between HPLC and UHPLC has not been done before. The adsorption isotherms of the four model compounds were determined for many different fractions of modifier. This is important because most analytical separations are conducted using gradient elution. Finally, data just from overloaded gradient elution experiments are used by the inverse method in gradient elution mode [18,19] to determine the adsorption isotherm and to predict overloaded gradient elution profiles for all model compounds, previously we have only studied uncharged and compounds described with type I (convex) adsorption isotherms.

This study is the first investigation in a series that aims to enhance the scientific knowledge needed for reliable analytical method transfer between HPLC and UHPLC using the Quality by Design (QbD) framework.

2 Theory

2.1 Equilibrium-dispersive model in gradient elution

To calculate band profiles, the equilibrium-dispersive (ED) model of chromatography [20] was used. It gives the following mass transport balance for component *i*:

$$\frac{\partial C_i}{\partial t} + F\frac{\partial q_i}{\partial t} + w\frac{\partial C_i}{\partial z} = D_a\frac{\partial^2 C_i}{\partial z^2} \tag{1}$$

where F is the phase ratio, w the superficial velocity of the mobile phase divided by the total porosity, D_a the apparent dispersion coefficient, t and z are the time and axial position and C and q are the mobile and stationary phase concentrations, respectively. D_a is calculated from the equation

$$D_a = \frac{wL}{2N} \tag{2}$$

where L is the column length and N the number of theoretical plates. When modelling single component band profiles in gradient elution we have that $q = q(C, C_M)$ where C is the solute concentration and C_M is the modifier concentration in the mobile phase, i.e. the system contains two components; the solute and the modifier. The initial condition was that the column was filled with pure mobile phase with the modifier fraction $C_{M,0}$. Danckwerts-type boundary conditions were used at the column inlet and outlet [21]. For the modifier the injection profile was described by

$$C_M(t, z=0) = \begin{cases} C_{M,0}, & 0 \le t < t_p \\ C_{M,0} + \beta(t - t_p), & t_p \le t < t_p + t_g \\ C_{M,0} + \Delta C_M, & t_p + t_g \le t \end{cases} \tag{3}$$

where t_p is the time when the gradient reaches the column inlet, t_g is the duration of the gradient, ΔC_M is the change in modifier fraction between the beginning and the end of the gradient and $\beta = \Delta C_M/t_g$ is the slope of the gradient. The injection profiles for the solutes were determined experimentally and fitted to empirical equations using non-linear regression (*see Appendix A*).

2.2 Adsorption Isotherm models in gradient elution

In this work the bi-Langmuir model,

$$q(C) = \frac{a_I C}{1 + b_I C} + \frac{a_{II} C}{1 + b_{II} C}, \tag{4}$$

best described the adsorption of BTEAC, C7 and SNS on BEH C18. a_I and a_{II} are the distribution constant for adsorption sites I and II and b_I and b_{II} are the association equilibrium constants for these sites. For OM the extended solid-liquid BET model [22] best fitted the data. The model takes into account adsorbate-adsorbate interactions and is written as

$$q(C) = \frac{aC}{(1 - b_L C)(1 - b_L C + bC)} \tag{5}$$

BET is just an expansion of the Langmuir adsorption model to multi-layer adsorption where b_L is the association equilibrium constant for surface adsorption-desorption over a layer of adsorbate molecules.

The following relationship has been suggested [23] between the retention factor, k, and the organic modifier, C_M, in reversed-phase LC

$$k(C_M) = k_w e^{-SC_M + dC_M^2} \tag{6}$$

where k_w is the retention factor in pure water. S and d describes how the retention factor changes with the organic modifier. In some cases, e.g. when a narrow range of modifier concentrations are considered, the d-term is omitted. Eq. (6) is also commonly used when describing how the adsorption isotherm parameters depend on the organic modifier [18,24]. Omitting the d-term the bi-Langmuir model is written as

$$q(C, C_M) = \frac{a_{I,0} e^{-S_{a_I} C_M} C}{1 + b_{I,0} e^{-S_{b_I} C_M} C} + \frac{a_{II,0} e^{-S_{a_{II}} C_M} C}{1 + b_{II,0} e^{-S_{b_{II}} C_M} C} \tag{7}$$

and the BET model becomes

$$q(C, C_M) = \frac{a_0 e^{-S_a C_M} C}{\left(1 - b_{L,0} e^{-S_{b_L} C_M} C\right)\left(1 - b_{L,0} e^{-S_{b_L} C_M} C + b_0 e^{-S_b C_M} C\right)}. \tag{8}$$

2.3 Determining adsorption isotherms in gradient elution

The inverse method is a method for acquiring adsorption data from few experiments with good agreement between the model and experiments [25]. In the inverse method, calculated band profiles are fitted directly to experimental ones using an optimization algorithm. Recently the inverse method was extended to gradient elution, i.e. modifier dependent adsorption isotherms were determined directly from overloaded bands obtained in gradient elution [18,19]. This simplifies considerably the otherwise tedious experimental procedure of modelling gradient elution in nonlinear LC and also enables acquisition of adsorption data from solutes that are very sensitive to the fraction of organic modifier in the eluent.

In the inverse method the adsorption isotherm is estimated by minimizing the sum of squared differences between experimental and calculated band profiles. In this study the minimization was done by a modified least squares Marquardt method [26] in three steps:

i. The column was assumed to work in analytical conditions and the parameters in the analytical version of the model, i.e. when b = 0, was estimated. This was done by minimizing the difference in retention time between experimental and calculated analytical peaks obtained at three different gradient slopes.
ii. Next the b-parameters were pre-estimated using the faster Rouchon algorithm to solve the mass balances, Eq. (1) on the base of four gradient elution, overloaded band profiles obtained at two different slopes.
iii. Finally all parameters in the modifier dependent adsorption isotherm were estimated simultaneously on the base of the same four overloaded band profiles.

In the previous studies [18,19] only uncharged compounds were investigated. In this study, anionic and cationic compounds which displayed stronger and more complex nonlinearity, was also studied along compound that the adsorption is described with a type III ("anti-Langmurian") adsorption isotherm.

3 Experimental

3.1 Chemicals

The mobile phase consisted of gradient grade acetonitrile purchased from VWR International (Radnor, PA, USA) and de-ionized water with conductivity 18.2 MΩ cm delivered from a Milli-Q Plus 185 water purification system from Merck Millipore (Billerica, MA, USA). For pycnometry dichloromethane, also purchased from VWR International, was used in combination with acetonitrile. The 30 mM phosphate buffer at pH 8.00 (22°C, ≈1 atm) was prepared from analytical grade sodium phosphate dibasic dihydrate and sodium phosphate monobasic dihydrate purchased from Sigma-Aldrich (St. Louis, MO, USA). The phosphate buffer was filtered through a 0.2 µm nylon filter membrane purchased from Whatman (Maidstone, UK) before use. Benzyltriethylammonium chloride "BTEAC" (99%), cycloheptanone "C7" (99%), sodium 2-naphtalenesulfonate "SNS" (≥95%), all from Sigma-Aldrich, and omeprazole sodium monohydrate "OM" (>99%), kindly gifted by AstraZeneca (Södertälje, Sweden), were used as solutes.

3.1.1 pH considerations

All experiments were performed with a phosphate buffer at ${}^{w}_{w}\mathrm{pH}$ = 8.00 and the ${}^{s}_{w}\mathrm{pH}$ in the mobile phase varied between 8.07 and 8.79 for 4 to 40% acetonitrile, respectively. The ${}^{w}_{w}\mathrm{pH}$ property is the pH measured and calibrated in aqueous solutions and the ${}^{s}_{w}\mathrm{pH}$ property is the pH measured in the organic aqueous mixtures and calibrated in aqueous solutions [27]. At these pH conditions BTEAC is positively charged, C7 is uncharged, SNS is negatively charged and OM (amphoteric compound, ${}^{w}_{w}\mathrm{p}K_{a,1}$ = 4.06 and ${}^{w}_{w}\mathrm{p}K_{a,2}$ = 0.79 [17]) is negatively charged. Phosphate buffers have been shown to keep pH relatively constant when temperature is changed moderately [28] so the temperatures effects of the pH was not considered further.

3.1.2 Sample preparation

Solutions of BTEAC, C7 and SNS were prepared by dissolving the pure compound directly in the eluent. In gradient elution the solvent was the same as the eluent at the start of the gradient. OM had low solubility in the eluent and was hard to dissolve directly in the eluent. Instead, solid OM was dissolved in

pure acetonitrile by heating the solution to 40°C. Then phosphate buffer, pre-heated to 40°C, was added and the solution was placed in an ultra-sonication bath until all solid particles were dissolved. Using this method the maximum solubility was ca. 1.1 g/L in 18% acetonitrile and 3 g/L in 30% acetonitrile and no precipitation was observed at room temperature at these concentrations. OM was stable in the mobile phase for approximately 24 h; hence all OM solution used in this work were prepared the same day as the chromatographic experiments were performed. All solutions were filtered through a 0.2 µm PTFE syringe filter purchased from Whatman (Maidstone, UK) before use.

3.2 HPLC instrumentation

The experiments denoted with HPLC were performed on an Agilent 1200 chromatograph (Agilent Technologies, Palo Alto, CA, USA) equipped with a binary pump, an auto sampler with a 900 µL loop, a diode-array UV-detector and a column thermostat. The temperature was 20°C and the flow rate was 1.00 mL/min. The dwell volume from the pump to the column inlet was 2.50 mL (determined according to ref. [29]) and the extra column volume from the auto sampler to the detector was 0.031 mL. The extra-column volumes were adjusted for in all experimental data. The HPLC column was a 100 × 4.6 mm XBridge C18 column with an average particle diameter of 3.5 µm. Two identical columns were used denoted XBridge #1 and XBridge #2. The column hold-up volumes, determined with pycnometry [30], were 0.991 mL and 1.011 mL for XBridge #1 and #2, respectively. XBridge #1 was used in all experiments except those with OM as solute. The columns were kindly supplied by Waters.

3.3 UHPLC instrumentation

The experiments denoted with UHPLC were performed on a Waters Acquity UPLC H-class (Waters Corporation, Milford, MA, USA) equipped with quaternary pump system, an auto sampler, a diode-array UV-detector (PDA according to Waters) and a column thermostat. The temperature was 40°C and the flow rate was 0.10 mL/min. At this flow rate the heat generation due to viscous friction is negligible. The dwell volume from the pump to the column inlet was 0.38 mL and the extra column volume from the auto sampler to the detector was 0.029 mL; the extra-column volumes were adjusted for in all experimental data. The UHPLC column was a 50 × 2.1 mm Acquity UPLC BEH C18 column with an average particle diameter of 1.7 µm. Two identical columns were used denoted BEH #1 and BEH #2. BEH #1 was used for all perturbation peak experiments and BTEAC elution profiles while BEH #2 was used for all other experiments. The columns were kindly gifted by Waters. The column hold-up volumes, determined with pycnometry [30], were 0.096 mL and 0.112 mL for the two BEH columns.

3.4 Adsorption isotherm measurements

3.4.1 Perturbation peaks

The Perturbation Peak (PP) method [20] was used for all components, except for OM, to obtain the adsorption energy distribution and adsorption isotherm for one fraction of modifier in the eluent. For BTEAC, perturbation pulses were introduced on 19 concentration plateaus ranging from 0 to 10 g/L at 5% acetonitrile in the mobile phase. For C7, perturbation pulses were introduced on 10 concentration plateaus ranging from 0 to 25 g/L at 25% acetonitrile in the mobile phase and for SNS perturbation pulses were introduced on 18 concentration plateaus ranging from 0 to 15 g/L at 15% acetonitrile in the mobile phase. The column was equilibrated for 30 min at each concentration plateau, replicate

perturbation peaks were recorded and the average retention time was used in the calculations of the adsorption data.

3.4.2 Frontal analysis

There were some problems to detect the perturbation peaks of OM at infinitesimally small disturbances using the PP method. Since the error in the PP method increases when there are large differences between the plateau concentration and that of the disturbances [31,32] the FA method was instead used for OM; 20 fronts were recorded between 0 and 2.5 g/L (which is the maximum solubility) at 25% acetonitrile in the mobile phase. An increase in pressure of 1 bar per front was observed in UHPLC which made frontal analysis of OM infeasible in UHPLC, therefore only FA-data for HPLC was obtained. The temperature was in this case changed to 30°C to lie between HPLC and UHPLC temperatures.

The reason for this increased pressure is probably because something in the omeprazole solution clogged the column; this is not surprising if we take into account the fact concentration of the solute (here OM) in frontal analysis sometimes exceeded thousand fold normal analytical levels. This increase in pressure was not observed when doing overloaded injection; only when pumping close to saturated solution through the system for longer times as was necessary in the FA experiments. The column could be regenerated by pumping 80/20 acetonitrile/water which agrees with the idea that the pressure increase are due to an impurity clogging the column.

3.4.3 Elution by characteristic points

To study how the adsorption isotherms depend on the fraction of organic modifier in the eluent, adsorption isotherm were determined at different fraction of organic modifier with the Elution by Characteristic points (ECP) method. The ECP only requires one overload elution profile for each condition and system as well as a calibration curve to be able to convert detector response to eluted concentration [20,33]. Overloaded band profiles in isocratic mode were obtained at five acetonitrile fractions. The acetonitrile fractions were different for the three solutes and chosen so that they covered the acetonitrile fractions used in the gradient mode. Three overloaded band profiles were recorded for each substance at each modifier fraction, giving a total of 45 overloaded band profiles for each system. The injection volume for UHPLC was scaled according to

$$V_{inj.}^{UHPLC} = V_{inj.}^{HPLC} \times \frac{V_{col.}^{UHPLC}}{V_{col.}^{HPLC}} \quad (9)$$

where $V_{inj.}$ is the injection volume and $V_{col.}$ is the geometric volume of the column [2].

3.4.4 Extended inverse method

The gradient experiments were performed by recording analytical and overloaded band profiles in gradient mode for three different linear gradients. Two overloaded profiles were recorded for each gradient and the gradients for each solute are shown in Table 1. Replicate measurements were done and the column was equilibrated with 20 column-volumes between successive gradient runs.

4 Computations

4.1 Adsorption energy distribution

The adsorption energy distribution (AED) is new tool for the chromatographic community to determine the number of different adsorption sites, and their different energy of interactions, before any rival model fit procedure. This information is useful when selecting the adsorption model to be fitted to the raw data; since we know the degree of column heterogeneity we can reduce the number of putative models to use in the rival model fitting procedure. This increases our understanding of the thermodynamics behind the retention mechanism. The adsorption energy distribution (AED) was calculated from raw slope data [34] acquired using ECP or perturbation peak method or raw adsorption data from frontal analysis experiments. In AED calculations we need to assume a local adoption isotherm model. In this study we used the Langmuir adsorption isotherm for all solutes showing type I adsorption (e.g. Langmuir) behavior. However, omeprazole showing type III adsorption behavior and we instead used the extended liquid-solid BET adsorption isotherm as local model [35,36]. In AED calculation we can only span the classical association, K, so we need to set the association equilibrium parameter between the adsorbate layers, b_L in Eq. (5) as a constant. In these calculations several different values of b_L were used to observe how it affects the AED, finally $b_L = 0.1$ were selected to be presented. In all calculations the expectation-maximization method [37], which does not require any a priori assumptions about the global adsorption isotherm, was used to compute the AED. One million iterations were used and the energy spaces were spanned with 400 grid points in the calculations. The adsorption energy boundaries were taken as $1/ (10 \times b_{max})$ and $10/b_{min}$.

4.2 ECP

The ECP method was used to determine adsorption isotherms for all different modifier fractions instead of FA and PP because ECP requires fewer experiments. In this study we used the slope ECP method, previously presented in [38]. Recently the slope ECP was also expanded and demonstrated to handle adsorption isotherm of type III (anti-Langmuirian) and adsorption isotherms with inflection points [39]. Using the ECP method it is necessary to have a calibration curve to convert detector response (R) to concentration (C). This was done by fitting the detector response for three different column loads for each condition to Eq. (10) so that the injected mass is equal to eluted mass.

$$C = k_1 \log\left(\frac{k_2}{k_2 - R}\right) \tag{10}$$

where k_1 and k_2 are constants. As a reference, the adsorption isotherms models determined using the FA and PP methods were used. Except for the UHPLC OM case where only ECP data were used due to experimental issues, discussed above.

4.3 Modeling of band profiles in gradient elution

The orthogonal collocation on finite elements method [40,41] was used to discretize the spatial derivatives of the ED model, Eq. (1), and the Adams-Moulton method implemented in the VODE procedure [42] was used to solve the system of ordinary differential equations. The number of subdomains was chosen as a tenth of the average column efficiency while the numerical accuracy was

fixed at 10^{-6}. The column efficiency was taken as the average efficiency at five isocratic levels spanning the gradient. This is a fair approximation because only the shape of heavily overloaded peaks, where the Shirazi number is high, was considered [20]. The total porosity, based on pycnometric measurements of the column hold-up volume, was assumed to be constant during the gradient run. This has been shown to be a good approximation for moderate changes in organic modifier [18].

5 Results and discussion

First the single component adsorption isotherm for each solute was determined at one acetonitrile fraction in the eluent in both HPLC and UHPLC. This was done with the PP method for all solutes except OM because perturbation peaks were difficult to detect for OM; instead the FA method was used for OM-HPLC. In OM-UHPLC the fronts increased the pressure so neither FA nor PP experiments were possible; instead the ECP method was used. Then the dependence of the organic modifier was studied and compared for HPLC and UHPLC. This was done by estimating the adsorption isotherms for five acetonitrile fractions in the eluent using the ECP method. Finally, the adsorption in gradient elution was studied using the inverse method and estimating modifier dependent adsorption isotherms directly from overloaded bands obtained in gradient elution.

5.1 Adsorption isotherms

The adsorption data were analyzed with a rigorous method prior to the model selection [43]. First Scatchard plots were constructed. Together with the shape of overloaded elution profiles, the type of adsorption could be determined. Overloaded band profiles having a sharp front and a diffuse rear is characteristic for type I ("Langmuir") models and a diffuse front and a sharp rear indicates type III ("anti-Langmuir") models. The adsorption was of type I for BTEAC, C7 and SNS, which was studied with the PP method, and the adsorption energy distribution (AED) was calculated from the raw slope data obtained using the Langmuir isotherm as the local adsorption model. OM showed type III adsorption and the adsorption data were determined using FA in the HPLC case and ECP in the UHPLC case. The AED for OM was calculated with the extended solid-liquid BET isotherm as the local adsorption model [35] using slope of the adsorption isotherm data for UHPLC and raw adsorption data in the HPLC case. The last step was the model selection which was done by fitting the adsorption isotherm models that were consistent with the observations from the Scatchard plot, overloaded band profiles and AED to the raw data with nonlinear regression.

BTEAC, which is positively charged, has overloaded band profiles of type I, a concave Scatchard plot and a bimodal AED with symmetrical distributions in both HPLC and UHPLC. The AED is shown in Fig. 1a. The adsorption energies and the saturation capacities for the adsorption sites are similar for HPLC and UHPLC. The bi-Langmuir model has a bimodal AED, is a type I adsorption isotherm with a concave Scatchard plot [43]. Using nonlinear regression, the bi-Langmuir model was fitted to the data, Fig. 1b. The model is consistent with all observations and fitted the data very well. The adsorption isotherms in HPLC and UHPLC are very close with the UHPLC isotherm slightly lower. The numerical fitting parameters in the bi-Langmuir models are presented in Table 2 and agree well with the AED calculations.

The uncharged solute (C7) showed overloaded band profiles of type I, a concave Scatchard plot which only had a slight curvature in UHPLC and a unimodal AED, Fig. 1c. Adsorption isotherm models that have one adsorption site and type I band profiles are the Langmuir, the Jovanovich and the Tóth isotherms [20]. The Jovanovich isotherm has a convex Scatchard plot and the Tóth model describes unsymmetrical unimodel energy distributions. Therefore the Langmuir model was fitted to the C7 data, but the fit was only moderate for HPLC, where the Scatchard plot had a more pronounced curvature, with an R^2 value of 0.9227 and only slightly better for UHPLC with R^2 equal to 0.9629. However, by adding a constant term to the Langmuir model,

$$q(C) = \frac{a_I C}{1 + b_I C} + a_{II} C \ , \tag{11}$$

excellent agreement between experiments and calculations could be achieved, see Fig. 1d. It should be noted that this is essentially the bi-Langmuir model with the b_{II}-term equal to zero, but since neither the Jovanovich nor the Tóth isotherms were consistent with all observations it was decided to keep Eq. (11). The difference between the adsorption isotherms in HPLC and UHPLC is largest at high concentrations, but it is still quite small even at 20 g/L.

The negatively charged solute (SNS) showed type I band profiles and concave Scatchard plots. The AED was bimodal in both HPLC in UHPLC, Fig. 1e. However, the high energy site had a very low saturation capacity in UHPLC. The adoption isotherms are described very well with the bi-Langmuir model for both HPLC and UHPLC conditions, see Fig. 1f. The difference in AED is also evident for the adsorption isotherms where the isotherm for UHPLC lies below the one corresponding to HPLC. The rather large difference in adsorption behavior between HPLC and UHPLC may be attributed to the temperature difference of 20°C between HPLC and UHPLC. The temperature dependence will be further investigated in a companion paper.

Omeprazole, which is also negatively charged, had a limited solubility and only a slight curvature could be seen on the adsorption isotherm. The overloaded band profiles was anti-Langmurian and the Scatchard plot was close to linear with a positive slope which is true for type III adsorption isotherms [43]. The AED calculation showed a single low energy site for both HPLC and UHPLC, Fig. 1g. The extended solid-liquid BET adsorption isotherm is consistent with these observation if $b_L \geq b/2$. The BET isotherm fitted the experimental data excellently with this condition fulfilled, Fig. 1h. Note that the UHPLC data is obtained with the ECP method at 40°C (hence no grey symbols in Fig. 1h) and that the FA data was acquired at 30 °C in HPLC. Note that for OM the UHPLC isotherm is above the HPLC counterpart which is the opposite from the model solutes. Overall, the AED and adsorption isotherm are very similar for HPLC and UHPLC.

In conclusion, no dramatic changes in the adsorption behavior were seen when comparing typical HPLC and UHPLC conditions. The heterogeneity was similar for the two stationary phases. One should expect similar adsorption characteristics when switching from HPLC to UHPLC and the same adsorption model could be used in HPLC and UHPLC.

5.2 Modifier dependence

Gradient elution is the most common programming technique in LC and is applied in a majority of the routine analysis. Therefore it is important to establish that the modifier dependence of the adsorption does not seriously change when going from HPLC to UHPLC. This was investigated on the basis of both analytical and overloaded peaks.

The relationship shown in Eq. (6) was found to describe the modifier dependence of the retention factor with excellent accuracy. In Table 3 the numerical parameters are listed for comparison and the result is plotted in Fig. 2. OM is the only solute where the k_w, S and d parameters differ by more than 10% between HPLC and UHPLC. The k_w parameter, which is the retention factor in pure water, should be reviewed critically in the case of OM and SNS because it is an extrapolation of the data and since these solutes are sensitive to the modifier fraction a small error in the experiments results in large errors in k_w. The S and d parameters explain how fast the retention factor changes with the modifier fraction. For OM the change is faster in HPLC. One reason for this is that the sensitivity increases with decreasing temperature. Another interesting feature is that retention factor for BTEAC decreases faster in HPLC conditions which gives a lower retention factor at 15% acetonitrile despite the higher temperature in UHPLC.

The adsorption model has been shown not to change with the fraction of organic modifier – only the numerical values of the parameters are affected [18,24]. Therefore the adsorption isotherm models found in Section 5.1 are assumed to be true at all modifier fractions and the numerical parameters are estimated with the ECP method for these models.

For BTEAC, Fig. 3, the b-parameters are generally larger in HPLC which is to expect when the temperature is lower. For HPLC, the modifier dependence is clearly not linear and the d-term must be used in Eq. (6). For the high energy site, site II, the a-parameters are almost identical for all investigated modifier fractions while the a-parameters for the low energy site, a_I, decreases more rapidly for HPLC which gives the faster decrease in retention time for HPLC seen in Fig. 2. For C7, Fig. 4, both a- and b-constants show very similar trends for HPLC and UHPLC. This indicates that neither the temperature nor the column chemistry results in any significant difference of the adsorption at any modifier fractions from an uncharged probes perspective. For SNS, Fig. 5, the a_{II}-constant for the high energy site, site II, is much higher for HPLC which can be correlated to the temperature difference between HPLC and UHPLC. One important observation is that the b-constants are significantly larger for UHPLC for acetonitrile fraction above 0.15 despite the higher temperature.

Due to the limited solubility of omeprazole, the concentration of the overloaded peak used in the ECP calculations are increasing from 1 g/L at 18% acetonitrile to 3 g/L at 30% acetonitrile. The trend for omeprazole, Fig. 6, is similar to those of BTEAC and C7 with equilibrium parameters which are lower for UHPLC. The most interesting feature in this case is the equilibrium constant, b_L, between solute layers. To our knowledge the dependence of organic modifier for this type of interaction has never been studied before. It seems like this equilibrium constant goes through a maximum when $k \simeq 10$. This is true for both HPLC and UHPLC and the maximum is almost at the same modifier fraction. Without data for other solutes, it is currently difficult to know if this is a unique feature for this solute or if it applies to other

type III adsorption isotherms. The adsorption isotherms for OM at the different modifier fractions are shown in Fig. 7. It is evident from the large difference between the isotherms that OM is very sensitive to the fraction of acetonitrile in the mobile phase. Changes in the acetonitrile fraction of only 2% result in a large change in the adsorption, especially at the lower fractions. The trend of the adsorption isotherms is almost identical in HPLC and UHPLC.

5.3 Modelling of gradient elution

The newly developed inverse method for gradient elution is, for the first time, used on ionic solutes and type III (anti-Langmuirian) adsorption isotherms. The aim is to model band profiles in gradient elution for both HPLC and UHPLC and predict overloaded band profiles in gradient elution but also to verify that the modelling methodology works for on ionic solutes and type III adsorption isotherms.

The modifier dependence of the adsorption parameters are investigated in Sec. 5.2 and fitted to Eq. (6) with the *d*-term included. The parameters estimated with the extended inverse method are empirical fitting parameters so the model should contain as few adjustable parameters as possible. Therefore, as a first approach the *d*-term in Eq. (6) is omitted when describing the modifier dependence of the adsorption parameters. See Eq. (7) and Eq. (8) for the models used in the gradient elution modelling.

Very good agreement between the calculated and experimental band profiles, which was used as a basis in the inverse method, could be achieved with the *d*-term in Eq. (6) omitted. The estimated models were then used to predict band profiles obtained at new gradient slopes and column loadings to verify their validity. The result is shown in Fig. 8 and it is evident that the estimations agree well with experiments for all cases. There were no significant differences in overlap for neither ionic solutes versus the uncharged one nor HPLC versus UHPLC. Note that the flow rate was kept low in the UHPLC experiments to avoid temperature gradients in the column. We conclude that both ionic solutes and type III models could successfully be modelled in gradient elution with the inverse method in gradient elution.

When the adsorption isotherms estimated in the inverse method are used to calculate the isocratic band profiles used in the ECP method, Sec. 5.2, excellent agreement was found in HPLC for all solutes. However, in UHPLC the isocratic band profiles were eluted slightly faster when the experimental ones. This is believed to be due an overestimation of the isocratic hold before the gradient reaches the column inlet, t_p in Eq. (3). Because the UHPLC is run at a very low flow rate, 0.1 mL/min, t_p is very sensitive to the estimation of the system volume between the pumps and the column inlet. This potential error is adjusted for automatically in the inverse method so all band profiles obtained in gradient elution are therefore well modelled. This hypothesis was investigated theoretically by calculating band profiles with known gradients and adsorption isotherms. These band profiles were then used as a basis for estimation by the inverse method with the column hold, t_p, overestimated by 15% and the gradient time, t_g, overestimated by 10%. Perfect agreement between estimated and true band profiles was obtained in gradient elution. However, if the estimated model was compared to the true band profiles in isocratic elution the overlap was only 90%, which is about the same as was seen for the UHPLC case described above.

We conclude that the inverse method in gradient elution works well for charge solutes and different types of adsorption isotherms. Accurate predictions can be made both in HPLC and UHPLC.

6 Conclusions

For the first time the adsorption differences and similarities between HPLC and UHPLC were investigated and modelled in detail using thermodynamics with state-of-the-art physicochemical theory. Four different solutes were investigated: one uncharged, one positively charged, one negatively charged and the negatively charged pharmaceutical compound omeprazole. The temperature, fraction of organic modifier and the particle size of the packing material were varied and a newly developed method for fast estimation of adsorption isotherms [18,19] in gradient elution mode was for the first time used with success for ionizable compounds and type- III adsorption isotherms.

The major conclusions are:

1) The adsorption isotherm model does not change when going from HPLC to UHPLC, only the values of the parameters. But the parameter dependence on fraction organic modifier is much more complicated, and complex, for charged compounds than for uncharged ones.
2) The adsorption energy distributions are similar for the HPLC and UHPLC stationary phases, although some differences in homogeneity was observed.
3) The dependence of the organic modifier followed the same trend in UHPLC as in HPLC.
4) The dependence of the organic modifier on a type-III adsorption isotherm, the solid-liquid BET model, was investigated for the first time. It was found that the equilibrium parameter for solute-solute layers had a maximum in both HPLC and UHPLC, which was independent of the temperature.

These conclusions indicate that there are small differences between the stationary phases used in HPLC and UHPLC and not any major changes in the adsorption mechanism of the solutes, i.e. change in peak shape or selectivity should be expecting due to differences in the stationary phases. This holds for both isocratic and gradient elution.

This study is the first in a series that aims to enhance the scientific knowledge needed for reliable analytical method transfer between HPLC and UHPLC using the Quality by Design (QbD) framework; the next studies will focus (i) on temperature effects and (ii) on practical implementations of the knowledge gained in this study in industrial analytical settings.

Acknowledgement

We are grateful to Waters that provided an ACQUITY UPLC H-Class system with support and technical advice during the project. We are also grateful to Anders Karlsson at AstraZeneca R&D Mölndal for initiating this project and for most valuable discussions. This work was supported by the Swedish Research Council (VR) in the project “Fundamental studies on molecular interactions aimed at

preparative separations and biospecific measurements" (grant number 621-2012-3978) and by (i) the Swedish Knowledge Foundation for the KK HÖG 2011 project "Improved Purification Processes to Satisfy Modern Drug Quality Assurance and Environmental Criteria" (grant number 20110212).

References

[1] S. Fekete, E. Oláh, J. Fekete, Fast liquid chromatography: The domination of core–shell and very fine particles, J. Chromatogr. A. 1228 (2012) 57–71.

[2] M. Szalka, J. Kostka, E. Rokaszewski, K. Kaczmarski, Analysis of related substances in bisoprolol fumarate on sub-2-µm adsorbents, Acta Chromatogr. 24 (2012) 163–183.

[3] S.A.C. Wren, P. Tchelitcheff, Use of ultra-performance liquid chromatography in pharmaceutical development, J. Chromatogr. A. 1119 (2006) 140–146.

[4] S. Fekete, J. Fekete, K. Ganzler, Validated UPLC method for the fast and sensitive determination of steroid residues in support of cleaning validation in formulation area, J. Pharm. Biomed. Anal. 49 (2009) 833–838.

[5] A.M. Evans, C.D. DeHaven, T. Barrett, M. Mitchell, E. Milgram, Integrated, Nontargeted Ultrahigh Performance Liquid Chromatography/Electrospray Ionization Tandem Mass Spectrometry Platform for the Identification and Relative Quantification of the Small-Molecule Complement of Biological Systems, Anal. Chem. 81 (2009) 6656–6667.

[6] R.N.O. Tettey-Amlalo, I. Kanfer, Rapid UPLC–MS/MS method for the determination of ketoprofen in human dermal microdialysis samples, J. Pharm. Biomed. Anal. 50 (2009) 580–586.

[7] A. Abrahim, M. Al-Sayah, P. Skrdla, Y. Bereznitski, Y. Chen, N. Wu, Practical comparison of 2.7 µm fused-core silica particles and porous sub-2 µm particles for fast separations in pharmaceutical process development, J. Pharm. Biomed. Anal. 51 (2010) 131–137.

[8] S. Fekete, I. Kohler, S. Rudaz, D. Guillarme, Importance of instrumentation for fast liquid chromatography in pharmaceutical analysis, J. Pharm. Biomed. Anal. In Press (2013).

[9] J. Musters, L. van den Bos, E. Kellenbach, Applying QbD Principles To Develop a Generic UHPLC Method Which Facilitates Continual Improvement and Innovation Throughout the Product Lifecycle for a Commercial API, Org. Process Res. Dev. 17 (2013) 87–96.

[10] A.S. Rathore, H. Winkle, Quality by design for biopharmaceuticals, Nat. Biotechnol. 27 (2009) 26–34.

[11] A. Rathore, R. Mahtre, Quality by Design for Biopharmaceuticals: Principles and Case Studies, Wiley, Hoboken, NJ, USA, 2009.

[12] M.M. Fallas, U.D. Neue, M.R. Hadley, D.V. McCalley, Further investigations of the effect of pressure on retention in ultra-high-pressure liquid chromatography, J. Chromatogr. A. 1217 (2010) 276–284.

[13] S. Fekete, J.-L. Veuthey, D.V. McCalley, D. Guillarme, The effect of pressure and mobile phase velocity on the retention properties of small analytes and large biomolecules in ultra-high pressure liquid chromatography, J. Chromatogr. A. 1270 (2012) 127–138.

[14] K. Kaczmarski, F. Gritti, J. Kostka, G. Guiochon, Modeling of thermal processes in high pressure liquid chromatography: II. Thermal heterogeneity at very high pressures, J. Chromatogr. A. 1216 (2009) 6575–6586.

[15] F. Gritti, M. Martin, G. Guiochon, Influence of Viscous Friction Heating on the Efficiency of Columns Operated under Very High Pressures, Anal. Chem. 81 (2009) 3365–3384.

[16] L. Olbe, E. Carlsson, P. Lindberg, A proton-pump inhibitor expedition: the case histories of omeprazole and esomeprazole, Nat. Rev. Drug Discov. 2 (2003) 132–139.

[17] J.M. Shin, Y.M. Cho, G. Sachs, Chemistry of Covalent Inhibition of the Gastric (H+, K+)-ATPase by Proton Pump Inhibitors, J. Am. Chem. Soc. 126 (2004) 7800–7811.
[18] D. Åsberg, M. Leśko, M. Enmark, J. Samuelsson, K. Kaczmarski, T. Fornstedt, Fast estimation of adsorption isotherm parameters in gradient elution preparative liquid chromatography. I: The single component case, J. Chromatogr. A. 1299 (2013) 64–70.
[19] D. Åsberg, M. Leśko, M. Enmark, J. Samuelsson, K. Kaczmarski, T. Fornstedt, Fast estimation of adsorption isotherm parameters in gradient elution preparative liquid chromatography II: The competitive case, J. Chromatogr. A. 1314 (2013) 70–76.
[20] G. Guiochon, D.G. Shirazi, A. Felinger, A.M. Katti, Fundamentals of preparative and nonlinear chromatography, 2nd ed., Academic Press, Boston, MA, 2006.
[21] P.V. Danckwerts, Continuous flow system, Chem. Eng. Sci. 2 (1953) 1–18.
[22] F. Gritti, W. Piatkowski, G. Guiochon, Comparison of the adsorption equilibrium of a few low-molecular mass compounds on a monolithic and a packed column in reversed-phase liquid chromatography, J. Chromatogr. A. 978 (2002) 81–107.
[23] P.J. Schoenmakers, H.A.H. Billiet, L. De Galan, Influence of organic modifiers on the rentention behaviour in reversed-phase liquid chromatography and its consequences for gradient elution, J. Chromatogr. A. 185 (1979) 179–195.
[24] P. Jandera, D. Komers, Fitting competitive adsorption isotherms to the experimental distribution data in reversed-phase systems, J. Chromatogr. A. 762 (1997) 3–13.
[25] E. Dose, S. Jacobson, G. Guiochon, Determination of isotherms from chromatographic peak shapes, Anal. Chem. 63 (1991) 833–839.
[26] R. Fletcher, A modified Marquardt sub-routine for non-linear least squares, Atomic Energy Research Establishment, Harwell, UK, 1971.
[27] M. Rosés, E. Bosch, Influence of mobile phase acid-base equilibria on the chromatographic behaviour of protolytic compounds, J. Chromatogr. A. 982 (2002) 1–30.
[28] L.G. Gagliardi, C.B. Castells, C. Ràfols, M. Rosés, E. Bosch, Effect of temperature on the chromatographic retention of ionizable compounds: II. Acetonitrile–water mobile phases, J. Chromatogr. A. 1077 (2005) 159–169.
[29] J.W. Dolan, Dwell Volume Revisited, LC GC N. A. 24 (2006) 458–466.
[30] F. Gritti, Y. Kazakevich, G. Guiochon, Measurement of hold-up volumes in reverse-phase liquid chromatography: Definition and comparison between static and dynamic methods, J. Chromatogr. A. 1161 (2007) 157–169.
[31] P. Forssén, J. Lindholm, T. Fornstedt, Theoretical and experimental study of binary perturbation peaks with focus on peculiar retention behaviour and vanishing peaks in chiral liquid chromatography, J. Chromatogr. A. 991 (2003) 31–45.
[32] J. Lindholm, P. Forssén, T. Fornstedt, Validation of the accuracy of the perturbation peak method for determination of single and binary adsorption isotherm parameters in LC, Anal. Chem. 76 (2004) 4856–4865.
[33] S. Ottiger, J. Kluge, A. Rajendran, M. Mazzotti, Enantioseparation of 1-phenyl-1-propanol on cellulose-derived chiral stationary phase by supercritical fluid chromatography. II. Non-linear isotherm, J. Chromatogr. A. 1162 (2007) 74–82.
[34] J. Samuelsson, T. Fornstedt, Calculations of the energy distribution from perturbation peak data--A new tool for characterization of chromatographic phases, J. Chromatogr. A. 1203 (2008) 177–184.
[35] M. Enmark, J. Samuelsson, T. Undin, T. Fornstedt, Characterization of an unusual adsorption behavior of racemic methyl-mandelate on a tris-(3,5-dimethylphenyl) carbamoyl cellulose chiral stationary phase, J. Chromatogr. A. 1218 (2011) 6688–6696.

[36] V. Agmo Hernández, J. Samuelsson, P. Forssén, T. Fornstedt, Enhanced interpretation of adsorption data generated by liquid chromatography and by modern biosensors, J. Chromatogr. A. 1317 (2013) 22–31.
[37] B.J. Stanley, G. Guiochon, Numerical estimation of adsorption energy distributions from adsorption isotherm data with the expectation-maximization method, J. Phys. Chem. 97 (1993) 8098–8104.
[38] J. Samuelsson, T. Undin, A. Törncrona, T. Fornstedt, Improvement in the generation of adsorption isotherm data in the elution by characteristic points method--The ECP-slope approach, J. Chromatogr. A. 1217 (2010) 7215–7221.
[39] J. Samuelsson, T. Undin, T. Fornstedt, Expanding the elution by characteristic point method for determination of various types of adsorption isotherms, J. Chromatogr. A. 1218 (2011) 3737–3742.
[40] J. Villadsen, M.L. Michelsen, Solution of Differential Equation Models by Polynomial Approximation, Prentice-Hall, Englewood Cliffs, NJ, 1978.
[41] K. Kaczmarski, M. Mazzotti, G. Storti, M. Mobidelli, Modeling fixed-bed adsorption columns through orthogonal collocations on moving finite elements, Comput. Chem. Eng. 21 (1997) 641–660.
[42] P.N. Brown, A.C. Hindmarsh, G.D. Byrne, Variable-Coefficient Ordinary Differential Equation Solver, available at: http://netlib.org.
[43] J. Samuelsson, R. Arnell, T. Fornstedt, Potential of adsorption isotherm measurements for closer elucidating of binding in chiral liquid chromatographic phase systems, J. Sep. Sci. 32 (2009) 1491–1506.

Figure captions

Fig. 1: Adsorption isotherms and calculated AED for BTEAC (circles), C7 (squares), SNS (diamonds) and OM (triangles) on HPLC (black symbols and lines) and UHPLC (gray symbols and lines). Lines in b), d), f) and h) are the best adsorption model fit. All AED were calculated using 10^6 iterations and energy space were spanned with 400 grid points.

Fig. 2: The retention factor as a function of fraction of acetonitrile (C_M) in the mobile phase is plotted. BTEAC (circles), C7 (squares), SNS (diamonds) and OM (triangles) on HPLC (black symbols and lines) and UHPLC (gray symbols and lines). The line represents a model fit to Eq. (6); see Table 3 for parameter values.

Fig. 3: The figure shows how the bi-Langmuir adsorption isotherm parameters, Eq. (5), depend on the modifier fraction for the adsorption of BTEAC in HPLC (black) and UHPLC (gray). Symbols are adsorption isotherm parameters determined using the ECP method. The lines are best model fit to Eq. (6).

Fig. 4: The figure shows how the Langmuir plus a linear term adsorption isotherm parameters, Eq. (11), depend on the modifier fraction for the adsorption of C7 in HPLC (black) and UHPLC (gray). Symbols are adsorption isotherm parameters determined using the ECP method. The lines are best model fit to Eq. (6). *See Appendix B for a Table with the numerical values of the adsorption isotherm parameters.*

Fig. 5: The figure shows how the bi-Langmuir adsorption isotherm parameters, Eq. (4), depend on the modifier fraction for the adsorption of SNS in HPLC (black) and UHPLC (gray). Symbols are adsorption

590 isotherm parameters determined using the ECP method. The lines are best model fit to Eq. (6). *See*
591 *Appendix B for a Table with the numerical values of the adsorption isotherm parameters.*

592 Fig. 6: The figure shows how the BET adsorption isotherm parameters, Eq. (5), depend on the modifier
593 fraction for the adsorption of OM in HPLC (black) and UHPLC (gray). Symbols are adsorption isotherm
594 parameters determined using the ECP method. The lines are best model fit to Eq. (6). *See Appendix B for*
595 *a Table with the numerical values of the adsorption isotherm parameters.*

596 Fig. 7: BET adsorption isotherms at different fraction of acetonitrile in the eluent in HPLC (black) and
597 UHPLC (gray) for OM. *See Appendix B for a Table with the numerical values of the adsorption isotherm*
598 *parameters.*

599 Fig. 8: Comparison between experimental (dashed lines) and predicted (solid lines) overloaded band
600 profiles in gradient elution. Grey lines are UHPLC and black lines are HPLC. The gradient slopes are 2, 3, 3
601 and 2%/min for BTEAC, C7, SNS and OM respectively. Note that these gradient slopes were not used in
602 the estimation of the model parameters. See Table 1 for further details.

Table 1: Experimental settings for the gradient experiments. C_{sample} is sample concentration, V_{inj} is injection volume and λ is detection wavelength. For other notation see Sec. 2.1.

Solute	BTEAC	BTEAC	C7	C7	SNS	SNS	OM	OM
System	HPLC	UHPLC	HPLC	UHPLC	HPLC	UHPLC	HPLC	UHPLC
C_{sample} **[g/L]**	5.00	5.00	25.00	25.63	5.00	5.00	1.00	1.00
V_{inj} **[µL]**	250, 500	25, 50	250, 500	25, 50	100, 200	6, 10, 12.5	300, 400, 500	30, 40, 50
$C_{M,0}$ **[%]**	4	4	15	15	7	7	18	18
ΔC_M **[%]**	26	26	25	25	18	18	12	12
t_p **[min]**	0.87	1.18	0.87	1.44	1.60	1.44	2.710	1.212
β **[%/min]**	1, 2, 3	1, 2, 3	1, 3, 5	1, 3, 5	1, 3, 5	1, 3, 5	1, 2, 3	1, 2, 3
λ **[nm]**	250	240	280	300	320	323	342	342

Table 2: Estimated adsorption isotherm parameters for BTEAC, C7 and SNS with the PP method. Parameters for OM were estimated with FA method in HPLC and ECP method in UHPLC.

Solute	**System**	a_I **[-]**	b_I **[L/g]**	a_{II} **[-]**	b_{II} **[L/g]**	b_L **[L/g]**
BTEAC	HPLC	3.72	0.198	11.8	3.82	-
BTEAC	UHPLC	3.22	0.157	8.34	3.12	-
C7	HPLC	3.93	0.0978	2.29	-	-
C7	UHPLC	3.56	0.0688	1.68	-	-
SNS	HPLC	1.38	0.0274	7.39	2.07	-
SNS	UHPLC	1.04	0.0213	4.09	1.55	-
OM	HPLC	7.37	2.27×10^{-5}	-	-	2.80×10^{-2}
OM	UHPLC	8.04	4.45×10^{-4}	-	-	2.85×10^{-2}

Table 3: Parameters estimation of Eq. (6) for $k(C_M)$.

Solute	**System**	R^2	k_w	S	d
BTEAC	HPLC	0.999	36.9	27.0	36.0
BTEAC	UHPLC	0.999	36.4	25.0	38.2
C7	HPLC	1.000	56.7	13.5	11.3
C7	UHPLC	1.000	52.6	12.9	10.5
SNS	HPLC	1.000	174	25.5	17.7
SNS	UHPLC	1.000	91.2	22.8	18.8
OM	HPLC	1.000	16.8×10^3	45.0	51.3
OM	UHPLC	1.000	4.22×10^3	37.1	38.6

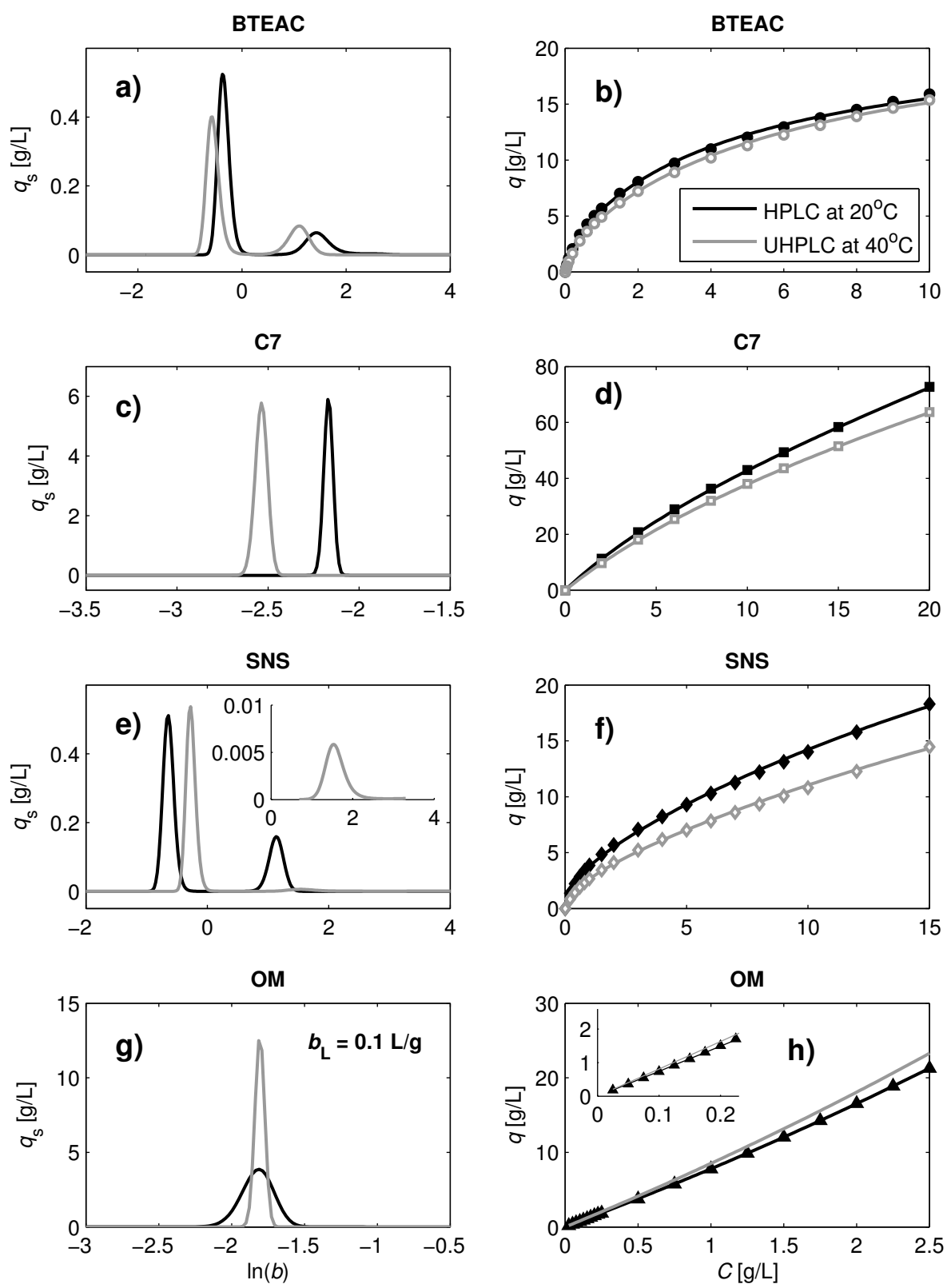
BTEAC
a)
q_s [g/L]
BTEAC
b)
q [g/L]
HPLC at 20°C
UHPLC at 40°C
C7
c)
q_s [g/L]
C7
d)
q [g/L]
SNS
e)
q_s [g/L]
SNS
f)
q [g/L]
OM
g)
b_L = 0.1 L/g
q_s [g/L]
ln(b)
OM
h)
q [g/L]
C [g/L]

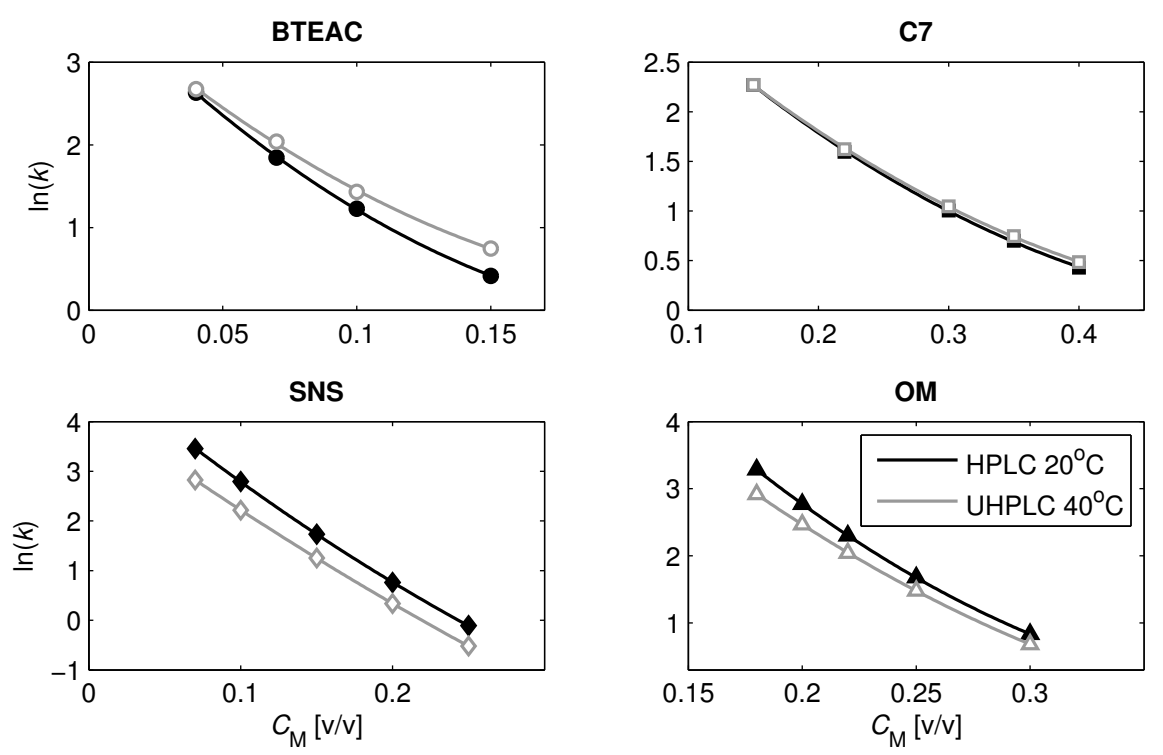
BTEAC
C7
SNS
OM
ln(k)
C_M [v/v]
HPLC 20°C
UHPLC 40°C

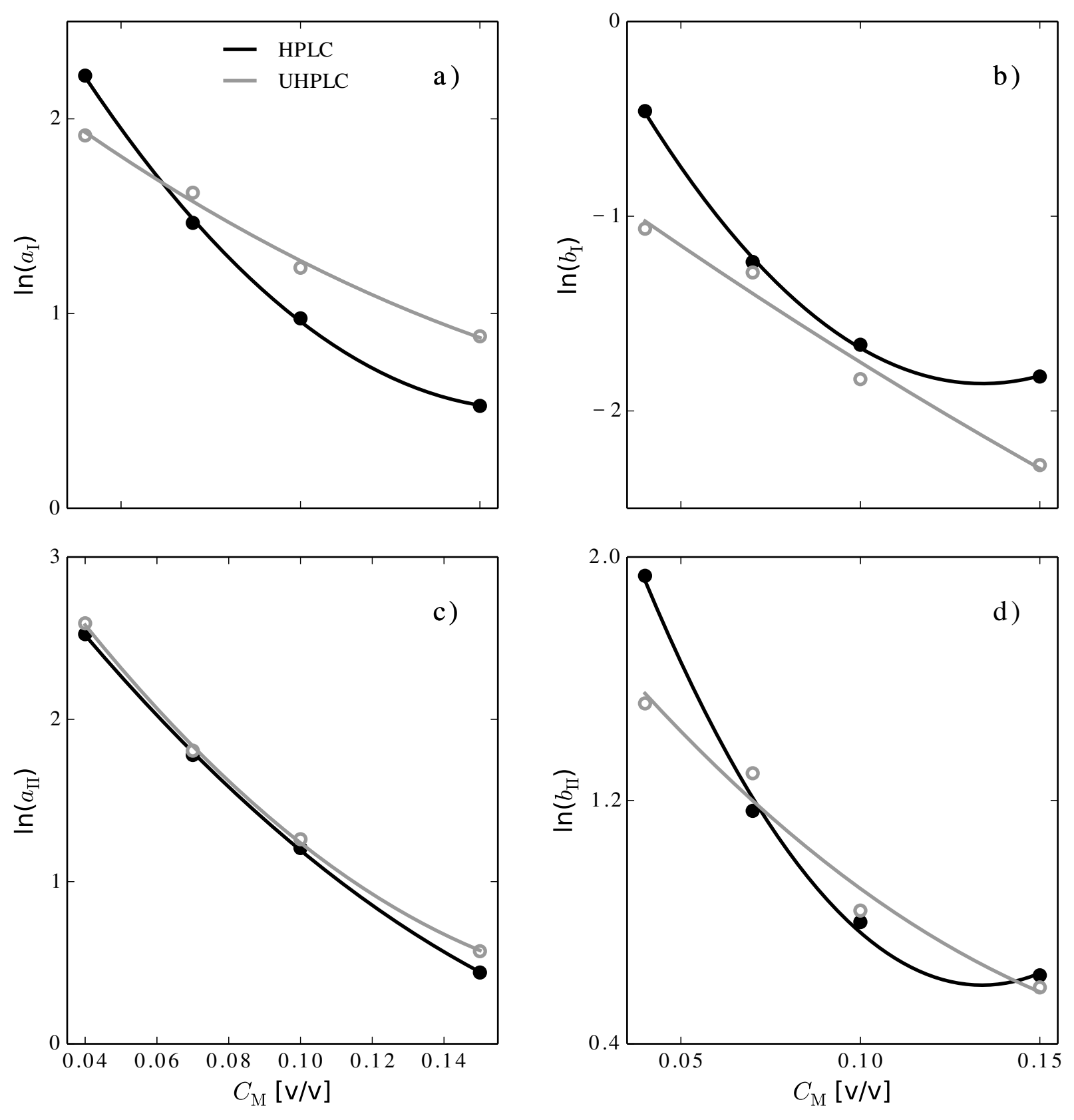
HPLC
UHPLC
a)
b)
c)
d)
ln(a_{I})
ln(b_{I})
ln(a_{II})
ln(b_{II})
C_{M} [v/v]
C_{M} [v/v]

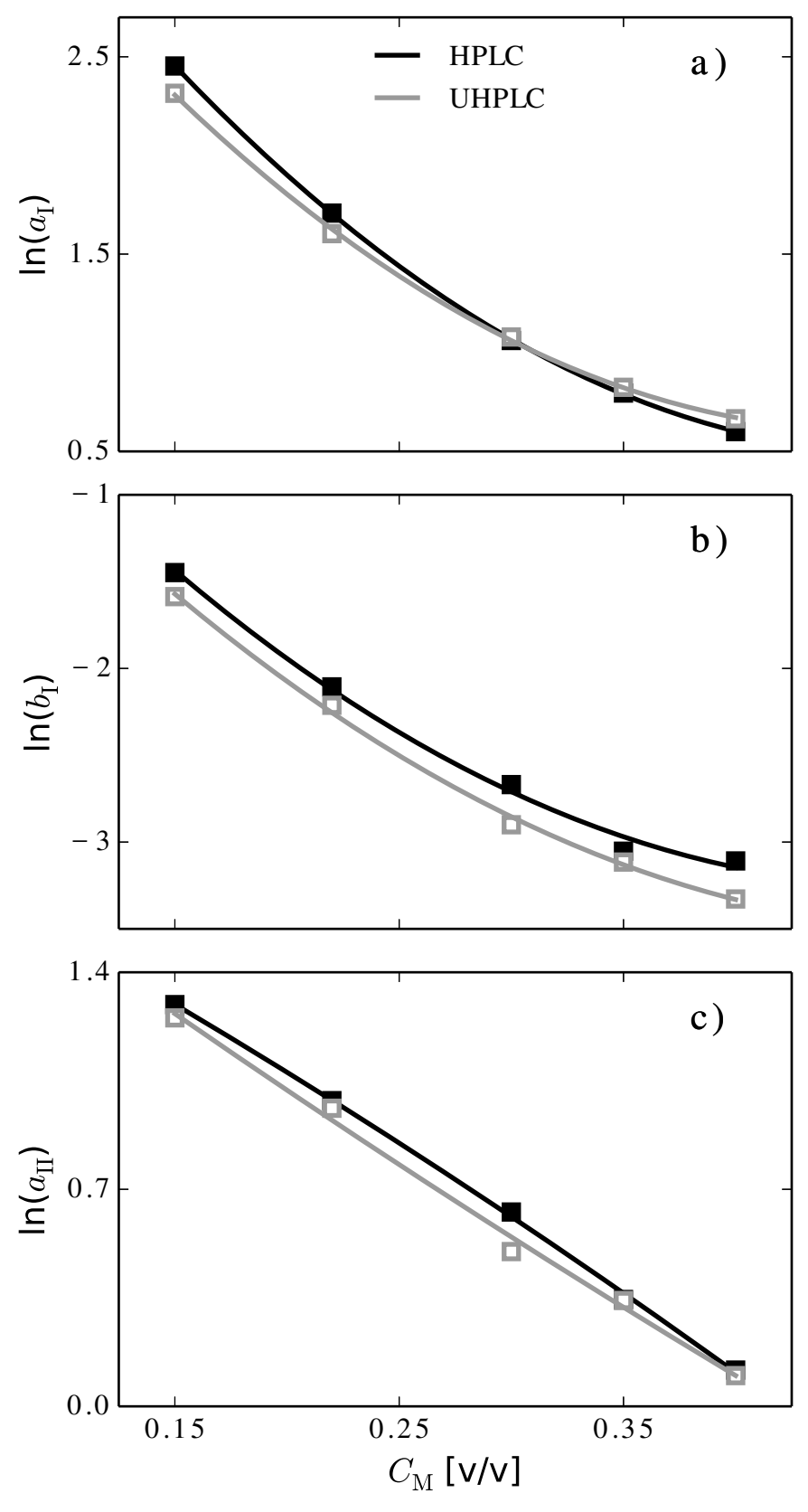
HPLC
UHPLC
a)
b)
c)
2.5
1.5
0.5
−1
−2
−3
1.4
0.7
0.0
0.15
0.25
0.35
ln(a_{I})
ln(b_{I})
ln(a_{II})
C_{M} [v/v]

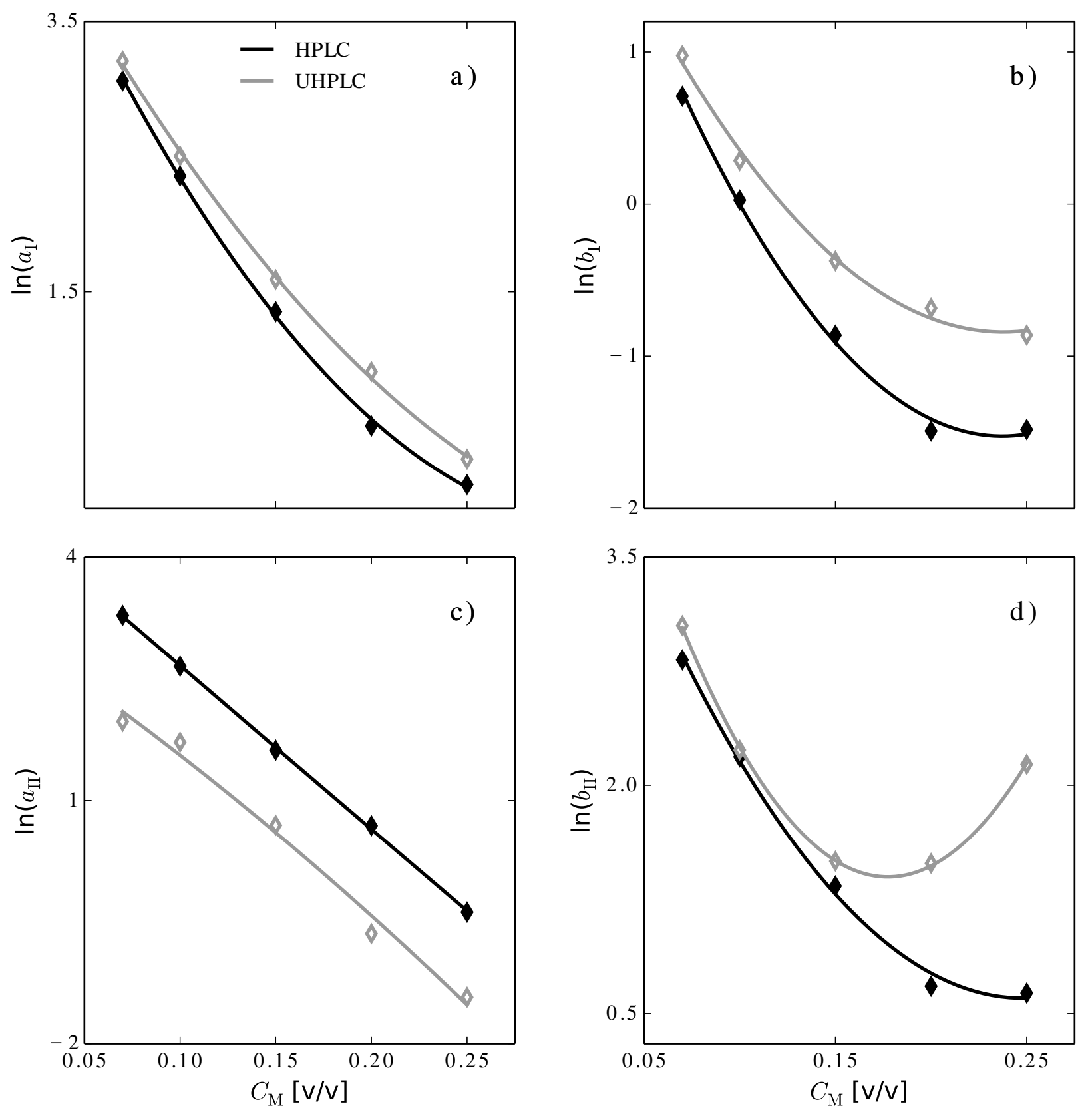
HPLC
UHPLC
a)
b)
c)
d)
ln(a_{I})
ln(b_{I})
ln(a_{II})
ln(b_{II})
C_{M} [v/v]
C_{M} [v/v]
3.5
1.5
1
0
−1
−2
4
1
−2
3.5
2.0
0.5
0.05
0.10
0.15
0.20
0.25
0.05
0.15
0.25

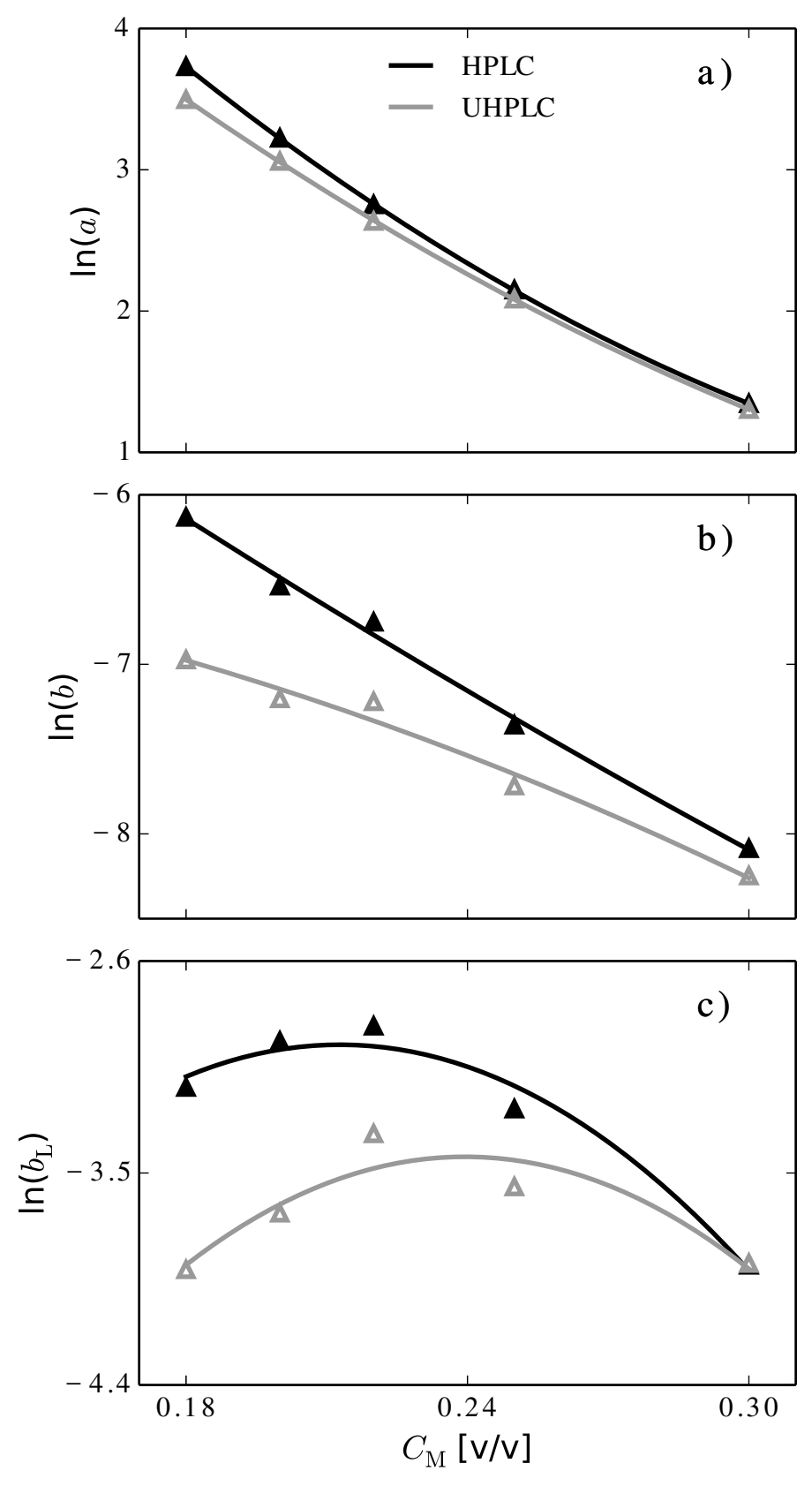
HPLC
UHPLC
a)
b)
c)
ln(a)
ln(b)
ln(b_L)
4
3
2
1
−6
−7
−8
−2.6
−3.5
−4.4
0.18
0.24
0.30
C_M [v/v]

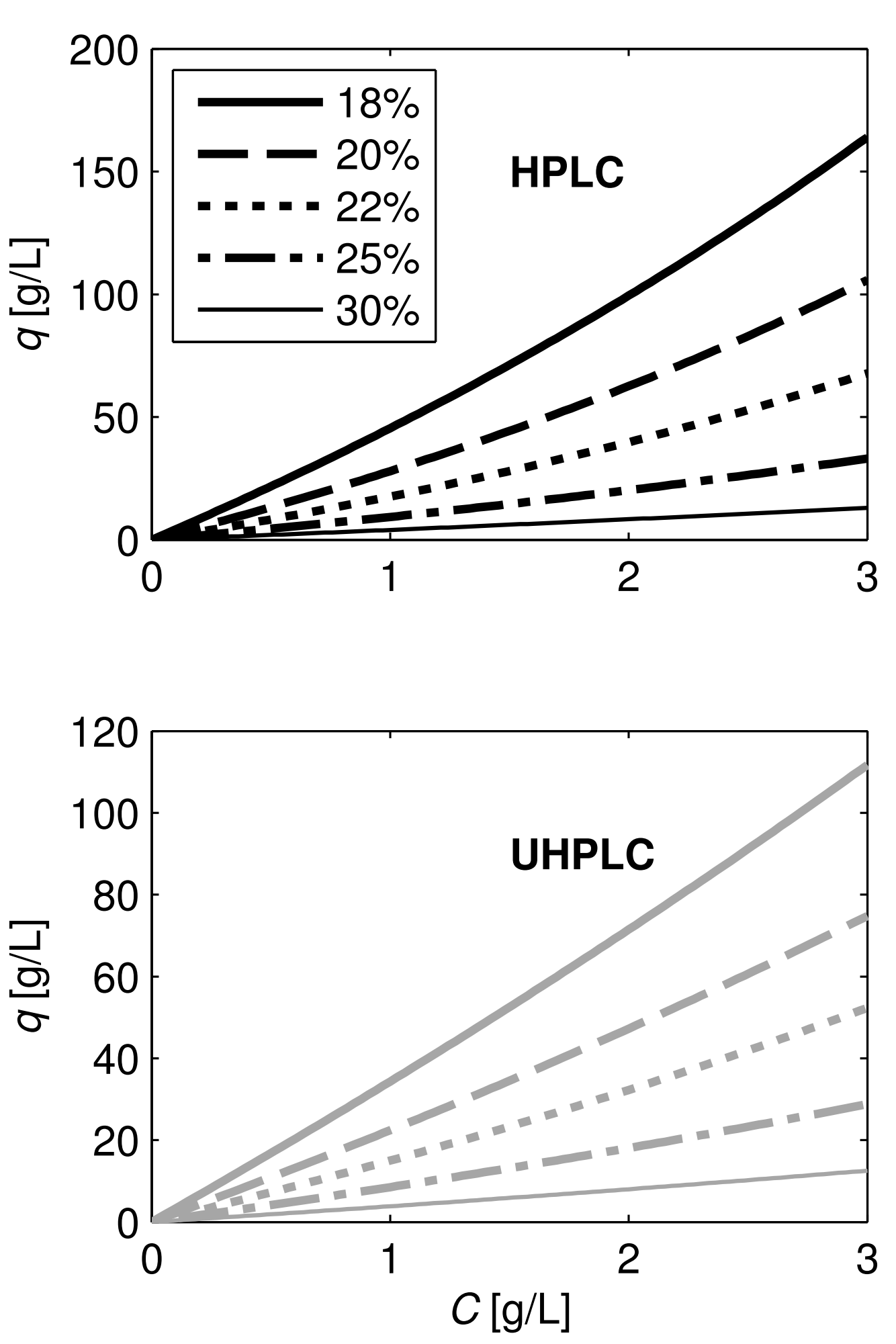
200
150
100
50
0
q [g/L]
18%
20%
22%
25%
30%
HPLC
0
1
2
3
120
100
80
60
40
20
0
q [g/L]
UHPLC
0
1
2
3
C [g/L]